Structural Monitoring and Maintenance, *Vol. 12*, *No. 4* (*2025*) *355-375*
https://doi.org/10.12989/smm.2025.12.4.355

Effect of longitudinal cracks on structural life of functionally graded beams exhibiting creep

Victor I. Rizov*[1] and Holm Altenbach[2]

[1]*Department of Technical Mechanics, University of Architecture, Civil Engineering and Geodesy, 1 Chr. Smirnensky blvd., 1046 – Sofia, Bulgaria*
[2]*Institute of Materials, Technologies and Mechanics, Fakultät für Maschinenbau, Otto-von-Guericke-Universität Magdeburg, Universitätsplatz 2, 39106 Magdeburg, Deutschland*

(*Received June 21*, *2025*, *Revised August 9*, *2025*, *Accepted August 11*, *2025*)

Abstract. Developing of approaches for evaluation of structural life of load-bearing functionally graded beam structures containing longitudinal cracks under creep is a current problem. This is due to the fact that in many cases longitudinal cracks are observed during routine maintenance check of such structures. The present paper novelty is that an approach for evaluating the effect of longitudinal cracks on structural life of functionally graded load-bearing beams which exhibit non-linear creep is developed. In this relation, general time-dependent solution of the strain energy release rate (SERR) is derived. The beams under consideration are functionally graded in the thickness direction. The crack is located arbitrary along the thickness. The creep behavior is described by non-linear stress-strain-time relationship written in general form. The solution of the SERR is derived by analyzing the time-dependent complementary strain energy. Two cases of behavior (beams with identical creep behavior in tension and compression and beams with asymmetrical creep behavior in tension and compression) are considered. The general solution is applied to evaluate the effect of a longitudinal crack on the structural life of a cantilever beam. The time-dependent SERR in the cantilever beam is obtained also by considering the balance of the energy for check-up of the general solution. It is found that the structural life is extended with increasing thickness to width ratio of the beam. However, the life of the structure is shortened as the crack length to beam length ratio increases. Furthermore, a beam with asymmetric creep behavior in tension and compression has a shorter structural life than that of a beam with identical creep behavior.

Keywords: functionally graded beam; longitudinal fracture; maintenance of structures; non-linear creep; structural life

1. Introduction

Functionally graded materials are continuously inhomogeneous composites which are made of two or more constituent materials (Njim *et al.* 2021, Mahamood and Akinlabi 2017, Markworth *et al*. 1995, Miyamoto *et al.* 1999, Rizov and Altenbach 2019, Udupa *et al*. 2014, Tokovyy and Ma 2019, Tokovyy 2019). The superior mechanical properties of functionally graded materials are

*Corresponding author, Professor, E-mail: V_RIZOV_FHE@UACG.BG
[a]Professor, E-mail: holm.altenbach@ovgu.de

http://www.techno-press.org/?journal=smm&subpage=7 ISSN: 2288-6605 (Print), 2288-6613 (Online)

achieved by gradually changing the composition of constituent materials along one or more spatial directions during the manufacturing process so that the interaction of the constituents would yield the desired material performance (Al-Shablle *et al.* 2022, Gasik 2010, Rizov 2020a). The fact that the properties of functionally graded materials can be formed technologically and vary continuously in the solid is one of the basic advantages of functionally graded materials over the conventional homogeneous structural materials (Hirai and Chen 1999, Kadum Njim *et al.* 2025, Mahamood and Akinlabi 2017, Markworth *et al*. 1995, Miyamoto *et al.* 1999, Nemat-Allal *et al.* 2011, Rizov 2024, Saiyathibrahim *et al*. 2016, Tokovyy and Ma 2017, Tokovyy and Ma 2021). Therefore, it is not surprising that the use of functionally graded materials for various advanced engineering applications in aeronautics, nuclear fusion reactors, engineering infrastructure, microelectronics, optics and biomedicine has increased in recent decades (Njim *et al.* 2021, Rizov 2025, Udupa *et al.* 2014, Tokovyy 2023, Tokovyy *et al.* 2025, Wu *et al*. 2014). In particular, the meaning of functionally graded load-bearing beams is essential. Beams are one of the most widely used structures in civil engineering (Ahmed *et al.* 2022, Ait Atmane *et al.* 2017, Daouadji *et al.* 2016, Sadoun *et al.* 2023).

The analysis of fracture provides very important information related to failure behavior and reliability of functionally graded materials and structural components (Dolgov 2024, Dowling 2013, Rizov 2020b, Rizov 2022). Normal functioning and in-service safety of structures depend in a high degree on their fracture behavior. Issues like extension of design life of structures and preve ntion of structural failures with purpose of minimizing the risk of loss of human lives and avoiding pollution of the environment are also related in some extent to fracture behavior and may be treated by using the methods of fracture mechanics. The continuous variation of the material properties in the volume of the solid makes the fracture analysis of functionally graded materials and structural components more complex in comparison with that of homogeneous materials and requires application of more sophisticated approaches. It should be noted further that functionally graded materials are frequently used for strengthening of load-bearing beam structures by external bonding of functionally graded strips (Daouadji *et al.* 2016, Sadoun *et al.* 2023). One of the problems here is the high risk of appearance of longitudinal cracks (debonding) between the beam and the strengthening strip. This fact also indicates the need for analysis of longitudinal failure behavior, especially when assessing the influence of longitudinal cracks on the life of beam structures.

There is a variety of problems in the area of fracture mechanics of functionally graded structural members and components which have to be treated more deeply. For example, analyses of longitudinal fracture in terms of the SERR in various functionally graded beam configurations subjected to different influences and loads are motivated by the fact that functionally graded materials can be built-up layer-by-layer (Mahamood and Akinlabi 2017) which is a premise for appearance of longitudinal cracks between layers. Another important moment in such analyses is the circumstance that very often members of engineering structures exhibit creep behaviour whose influence has to be taken into account (Nguyen *et al.* 2015, Nguyen *et al.* 2020, Nguyen *et al.* 2025, Truong *et al.* 2024).

It is known from the engineering practise that in some cases longitudinal cracks are observed during routine maintenance check of various load-bearing functionally graded structures under prolonged loading. The presence of such cracks undoubtedly represents a significant treat for functioning and safety of structures. When dealing with a situation in which a longitudinal crack is observed, there are many questions that have to be considered carefully. For instance, one of these questions is about the effect of the longitudinal crack on the structural life.

In this relation, the aim of this paper is to develop an approach that can be applied for evaluation of the structural life at the presence of longitudinal crack in functionally graded beam configurations exhibiting non-linear creep. For achieving of this aim, general time-dependent solution of the SERR in functionally graded load-bearing beam structures which exhibit non-linear creep behavior is derived here. The beams under consideration are functionally graded in the thickness direction. The mechanical behavior of the beam is described by a general non-linear stress-strain-time relationship. Two cases (beams with identical creep behavior in tension and compression and beams with asymmetrical creep behavior in tension and compression) are considered in this paper. The general solution is applied to obtain the time-dependent SERR for a functionally graded cantilever beam under non-linear creep. The time-dependent SERR in the cantilever beam is derived also by analyzing the balance of the energy for verification. The variation of the SERR with time induced by the creep behavior is evaluated. It is shown how the general solution of the SERR can be applied for determining the structural life. The influence of a variety of factors like external loading, crack length, beam geometry and asymmetrical non-linear creep behavior in tension and compression on the structural life is studied and illustrated by different graphs.

2. Beams with identical creep behavior in tension and compression

Functionally graded beams with a longitudinal crack exhibiting creep are under consideration. A beam portion with the crack tip is shown schematically in Fig. 1.

The cross-section of the beam is a rectangle of width, b, and thickness, h. The crack is located arbitrary along the beam thickness. The thicknesses of the lower and the upper crack arms are denoted by h_1 and h_2, respectively (Fig. 1). The beam is under combination of bending moment, M, and axial force, N. According to (Rizov 2020a) the SERR, G, can be written as

$$G=\int_{-\frac{h_1}{2}}^{\frac{h_1}{2}} u_{01}^{*} dz_1 + \int_{-\frac{h_2}{2}}^{\frac{h_2}{2}} u_{02}^{*} dz_2 - \int_{-\frac{h}{2}}^{\frac{h}{2}} u_{03}^{*} dz_3 \tag{1}$$

where u_{01}^{*}, u_{02}^{*} and u_{03}^{*} are, respectively, the complementary strain energy densities in the lower and the upper crack arms behind the crack tip and in the un-cracked portion of the beam ahead of the crack tip, z_1, z_2 and z_3 are the vertical centroidal axes of the cross-sections of the lower and the upper crack arms and the un-cracked portion of the beam, respectively.

The complementary strain energy density in the lower crack arm is expressed as (Rizov 2020a)

$$u_{01}^{*} = \sigma\varepsilon - u_{01} \tag{2}$$

where σ is the stress, ε is the strain. The strain energy density, u_{01}, is written as

$$u_{01} = \int_{0}^{\varepsilon} \sigma d\varepsilon \tag{3}$$

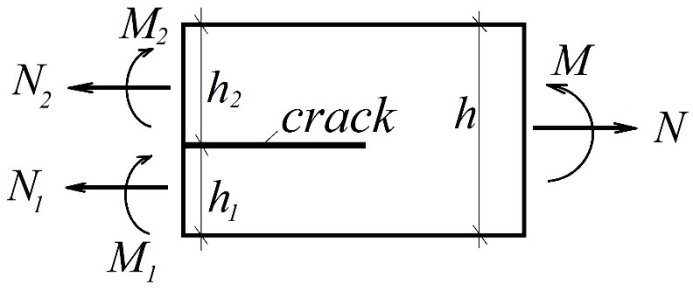

Fig. 1. Portion of a beam with the crack tip

In order to calculate u_{01} by using (3), one needs a stress-strain relationship. Since the material under consideration exhibits non-linear creep behavior, a non-linear stress-strain-time relationship written in a general form is used in the present analysis

$$\varepsilon = f(\sigma, t) \tag{4}$$

where t is the time, $f(\sigma,t)$ is a non-linear function of the stress and the time.

The distribution of ε in the cross-section of the lower crack arm is written as

$$\varepsilon = \kappa_1 (z_1 - z_{1n}) \tag{5}$$

where κ_1 is the curvature, z_{1n} is the coordinate of the neutral axis. The following approach is applied to determine the curvature and the coordinate of the neutral axis. First, the equation for equilibrium of the cross-section of the lower crack arm are written as

$$N_1 = b \int_{-\frac{h_1}{2}}^{\frac{h_1}{2}} \sigma dz_1 \tag{6}$$

$$M_1 = b \int_{-\frac{h_1}{2}}^{\frac{h_1}{2}} \sigma z_1 dz_1 \tag{7}$$

where N_1 and M_1 are the axial force and the bending moment in the cross-section of the lower crack arm behind the crack tip. In order to perform the integration in (6) and (7), σ has to expressed in a function of z_1. For this purpose, (5) is substituted in (4)

$$\kappa_1 (z_1 - z_{1n}) = f(\sigma, t) \tag{8}$$

However, in general case, σ can not be determined explicitly from Eq. (8) due to the non-linear character of the function, $f(\sigma,t)$. Therefore, σ is expanded in series of Maclaurin by retaining of the first three members

$$\sigma(z_1) \approx \sigma(0) + \frac{\sigma'(0)}{1!} z_1 + \frac{\sigma''(0)}{2!} z_1^2 . \tag{9}$$

Expression (9) is rewritten as

$$\sigma(z_1) \approx \beta + \delta z_1 + \eta z_1^2 \tag{10}$$

where β, δ and η are unknown coefficients. By substituting of (10) in (6) and (7), one obtains

$$N_1 = b\beta h_1 + \frac{1}{12} b\eta h_1^3 \tag{11}$$

$$M_1 = \frac{1}{12} b\delta h_1^3 . \tag{12}$$

There are three unknowns, β, δ and η, in Eqs. (11) and (12). In order to determine the unknowns, we compose additional equations. For this purpose, first, (10) is substituted in (8). Then, by substituting of $z_1 = 0$ in (8) and in the first and the second derivatives of (8) with respect to z_1 one obtains

$$-\kappa_1 z_{1n} = f(\sigma, t)_{at\ z_1=0} \tag{13}$$

$$\kappa_1 = f'(\sigma, t)_{at\ z_1=0} \tag{14}$$

$$0 = f''(\sigma, t)_{at\ z_1=0} \tag{15}$$

Besides β, δ and η, two other unknowns, namely κ_1 and z_{1n} appear in (13), (14) and (15). Eqs. (11)-(15) can be solved with respect to κ_1, z_{1n}, β, δ and η for particular function, $f(\sigma, t)$, law for distribution of the properties of the functionally graded material along the thickness of the beam and values of the bending moment and the axial force. Then, u_{01}^* and u_{01} can be obtained by substituting of (10) in (2) and (3).

The complementary strain energy density in the upper crack arm that is involved in (1) is found by using (2). For this purpose, σ, ε and u_{01} are replaced, respectively, with σ_{up}, ε_{up} and u_{02} where σ_{up} is the stress, ε_{up} is the strain and u_{02} is the strain energy density in the upper crack arm. The stress, σ_{up}, is obtained by replacing of z_1, β, δ and η with z_2, β_{up}, δ_{up} and η_{up} in (10). Eqs. (11)-(15) are used to determine κ_2, z_{2n}, β_{up}, δ_{up} and η_{up} (here, κ_2 is the curvature, z_{2n} is coordinate of the neutral axis of the upper crack arm). For this purpose, N_1, M_1, κ_1, z_{1n}, β, δ and η are replaced, respectively, with N_2, M_2, κ_2, z_{2n}, β_{up}, δ_{up} and η_{up} where N_1 and M_1 are the axial force and the bending moment in the upper crack arm, respectively.

The complementary strain energy density in the un-cracked beam portion ahead of the crack tip is calculated by replacing of σ, ε and u_{01}, respectively, with σ_{un}, ε_{un} and u_{03} in formula (2). Here, σ_{un}, ε_{un} and u_{03} are the stress, the strain and the strain energy density in the un-

cracked beam portion, respectively. Formula (10) is used to obtain σ_{un}. For this purpose, z_1, β, δ and η are replaced, respectively, with z_3, β_{un}, δ_{un} and η_{un}. The unknowns, κ_3, z_{3n}, β_{un}, δ_{un} and η_{un}, (here κ_3, z_{3n} are the curvature and the coordinate of the neutral axis) are determined from Eqs. (11)-(15). For this purpose, N_1, M_1, κ_1, z_{1n}, β, δ and η are replaced with N, M, κ_3, z_{3n}, β_{un}, δ_{un} and η_{un}, respectively.

The SERR can be obtained by substituting of the complementary strain energy densities in (1).

3. Beams with asymmetrical creep behavior in tension and compression

In order to derive the SERR for the crack problem in Fig. 1 when the beam exhibits asymmetrical creep behavior in tension and compression, formula (1) is re-written as

$$G=\int\limits_{-\frac{h_1}{2}}^{z_{1n}} u_{01c}^{*}dz_1+\int\limits_{z_{1n}}^{\frac{h_1}{2}} u_{01t}^{*}dz_1+\int\limits_{-\frac{h_2}{2}}^{z_{2n}} u_{02c}^{*}dz_2+\int\limits_{z_{2n}}^{\frac{h_1}{2}} u_{02t}^{*}dz_2-\int\limits_{-\frac{h}{2}}^{z_{3n}} u_{03c}^{*}dz_3-\int\limits_{z_{3n}}^{\frac{h}{2}} u_{03t}^{*}dz_3, \tag{16}$$

where u_{01c}^{*}, u_{01t}^{*}, u_{02c}^{*}, u_{02t}^{*}, u_{03c}^{*} and u_{03t}^{*} are the complementary strain energy densities in the compression and the tension zones of the cross-sections of the lower and the upper crack arms behind the crack tip and in the un-cracked portion of the beam ahead of the crack tip.

The complementary strain energy densities in the compression and the tension zones of the cross-section of the lower crack arm are obtained as

$$u_{01c}^{*}=\sigma_c\varepsilon-u_{01c} \tag{17}$$

$$u_{01t}^{*}=\sigma_t\varepsilon-u_{01t} \tag{18}$$

where σ_c and σ_t are the stresses in compression and tension, respectively. The strain energy densities in compression and tension, u_{01c} and u_{01t}, are expressed as

$$u_{01c}=\int\limits_0^{\varepsilon}\sigma_c d\varepsilon. \tag{19}$$

$$u_{01t}=\int\limits_0^{\varepsilon}\sigma_t d\varepsilon. \tag{20}$$

The stress-strain-time relationships in compression and tension which are needed in order to calculate the complementary strain energy densities are written, respectively, as

$$\varepsilon=f(\sigma_c,t) \tag{21}$$

and

$$\varepsilon=f(\sigma_t,t) \tag{22}$$

Since the position of the neutral axis is not known in advance, the stresses, σ_c and σ_t, are expanded in series of Taylor

$$\sigma_c(z_1) \approx \beta_c + \delta_c(z_1 - z_{1c}) + \eta_c(z_1 - z_{1c})^2 \tag{23}$$

$$\sigma_t(z_1) \approx \beta_t + \delta_t(z_1 - z_{1t}) + \eta_t(z_1 - z_{1t})^2 \tag{24}$$

where $z_{1c} = (-h_1 + z_{1n})/2$, $z_{1t} = (h_1 - z_{1n})/2$. It should be noted that $-h_1/2 \le z_1 \le z_{1n}$ and $z_{1n} \le z_1 \le h_1/2$ in (23) and (24), respectively. In order to determine the coefficients, β_c, δ_c, η_c, β_t, δ_t and η_t, the equations for equilibrium of the cross-section of the lower crack arm are written as

$$N_1 = b\int_{-\frac{h_1}{2}}^{z_{1n}} \sigma_c dz_1 + b\int_{z_{1n}}^{\frac{h_1}{2}} \sigma_t dz_1, \tag{25}$$

$$M_1 = b\int_{-\frac{h_1}{2}}^{z_{1n}} \sigma_c z_1 dz_1 + b\int_{z_{1n}}^{\frac{h_1}{2}} \sigma_t z_1 dz_1. \tag{26}$$

By substituting of (23) and (24) in (25) and (26), one obtains

$$\begin{aligned} N_1 = b\Bigg\{ & \beta_c\left(z_{1n} + \frac{h_1}{2}\right) + \frac{\delta_c}{2}\left[(z_{1n} - z_{1c})^2 - \left(-\frac{h_1}{2} - z_{1n}\right)^2\right] + \frac{\eta_c}{3}\left[(z_{1n} - z_{1c})^3 - \left(-\frac{h_1}{2} - z_{1c}\right)^3\right]\Bigg\} + \\ + b\Bigg\{ & \beta_t\left(\frac{h_1}{2} - z_{1n}\right) + \frac{\delta_t}{2}\left[\left(\frac{h_1}{2} - z_{1t}\right)^2 - (z_{1n} - z_{1t})^2\right] + \frac{\eta_t}{3}\left[\left(\frac{h_1}{2} - z_{1t}\right)^3 - (z_{1n} - z_{1t})^3\right]\Bigg\} \end{aligned} \tag{27}$$

$$\begin{aligned} M_1 = b\Bigg\{ & \frac{\beta_c}{2}\left(z_{1n}^2 - \frac{h_1^2}{4}\right) + \delta_c\left[\frac{1}{3}\left(z_{1n}^3 + \frac{h_1^3}{8}\right) - \frac{z_{1c}}{2}\left(z_{1n}^2 - \frac{h_1^2}{4}\right)\right] + \\ & + \eta_c\left[\frac{1}{4}\left(z_{1n}^4 - \frac{h_1^4}{16}\right) - \frac{2z_{1c}}{3}\left(z_{1n}^3 + \frac{h_1^3}{8}\right) + \frac{z_{1c}^2}{2}\left(z_{1n}^2 - \frac{h_1^2}{4}\right)\right]\Bigg\} + \\ & + b\Bigg\{ \frac{\beta_t}{2}\left(\frac{h_1^2}{4} - z_{1n}^2\right) + \delta_t\left[\frac{1}{3}\left(\frac{h_1^3}{8} - z_{1n}^3\right) - \frac{z_{1t}}{2}\left(\frac{h_1^2}{4} - z_{1n}^2\right)\right] + \\ & + \eta_t\left[\frac{1}{4}\left(\frac{h_1^4}{16} - z_{1n}^4\right) - \frac{2z_{1t}}{3}\left(\frac{h_1^3}{8} - z_{1n}^3\right) + \frac{z_{1t}^2}{2}\left(\frac{h_1^2}{4} - z_{1n}^2\right)\right]\Bigg\} \end{aligned} \tag{28}$$

Further six equations are written in the following way. First, (23) and (24) are substituted in (21) and (22), respectively. Then, by substituting of $z_1 = z_{1c}$ in (21) and in the first and the second derivatives of (21) with respect to z_1, one obtains

$$\kappa_1(z_{1c} - z_{1n}) = f(\sigma_c, t)_{at\ z_1 = z_{1c}} \tag{29}$$

$$\kappa_1 = f'(\sigma_c, t)_{at\ z_1=z_{1c}} \tag{30}$$

$$0 = f''(\sigma_c, t)_{at\ z_1=z_{1c}} \tag{31}$$

Analogically, by substituting of $z_1 = z_{1t}$ in (22) and in the first and the second derivatives of (22) with respect to z_1, one arrives at

$$\kappa_1(z_{1t} - z_{1n}) = f(\sigma_t, t)_{at\ z_1=z_{1t}} \tag{32}$$

$$\kappa_1 = f'(\sigma_t, t)_{at\ z_1=z_{1t}} \tag{33}$$

$$0 = f''(\sigma_t, t)_{at\ z_1=z_{1t}} \tag{34}$$

Eqs. (27)-(34) can be solved with respect to κ_1, z_{1n}, β_c, δ_c, η_c, β_t, δ_t and η_t for particular functions, $f(\sigma_c, t)$ and $f(\sigma_t, t)$, material properties and values of N_1 and M_1. Then, the energy densities are found by substituting of (23) and (24) in (17)-(20).

Formulae (17) and (18) are applied also to obtain the complementary strain energy densities in the compression and tension zones of the cross-section of the upper crack arm behind the crack tip. For this purpose, σ_c, σ_t, ε, u_{01c} and u_{01t} are replaced, respectively, with σ_{upc}, σ_{upt}, ε_{up}, u_{02c} and u_{02t} where σ_{upc} and σ_{upt} are the stresses in the compression and tension zones, ε_{up} is the strain, u_{02c} and u_{02t} are the complementary strain energy densities in the compression and the tension zones of the upper crack arm. The unknowns, κ_2, z_{2n}, β_{upc}, δ_{upc}, η_{upc}, β_{upt}, δ_{upt} and η_{upt} are obtained by using Eqs. (27)-(34). For this purpose, N_1, M_1, κ_1, z_{1n}, β_c, δ_c, η_c, β_t, δ_t and η_t are replaced with N_2, M_2, κ_2, z_{2n}, β_{upc}, δ_{upc}, η_{upc}, β_{upt}, δ_{upt} and η_{upt}, respectively.

The complementary strain energy densities in the compression and the tension zones of the un-cracked beam portion ahead of the crack tip are derived by replacing of σ_c, σ_t, ε, u_{01c} and u_{01t} with σ_{unc}, σ_{unt}, ε_{un}, u_{03c} and u_{03t} in (17) and (18) where σ_{unc} and σ_{unt} are the stresses in the compression and the tension zones, ε_{un} is the strain, u_{03c} and u_{03t} are the complementary strain energy densities in the compression and the tension zones of the cross-section of the un-cracked beam portion ahead of the crack tip. Equations (27) – (34) are used to determine κ_3, z_{3n}, β_{unc}, δ_{unc}, η_{unc}, β_{unt}, δ_{unt} and η_{unt}. For this purpose, N_1, M_1, κ_1, z_{1n}, β_c, δ_c, η_c, β_t, δ_t and η_t are replaced, respectively, with N, M, κ_3, z_{3n}, β_{unc}, δ_{unc}, η_{unc}, β_{unt}, δ_{unt} and η_{unt}.

The complementary strain energy densities have to be substituted in (16) to calculate the SERR.

It should be noted that the general solutions of the SERR derived in the present paper are time-dependent on account of creep behaviour. The solutions can be applied to calculate the SERR with taking into account the non-linear creep behavior at various values of the time.

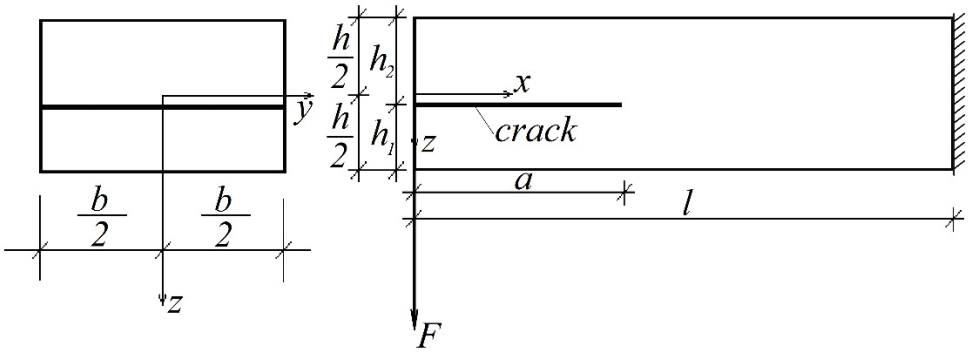

Fig. 2 The geometry and loading of a cantilever beam with a longitudinal crack

4. Illustrative example

The general solution derived in the previous section of the paper is applied here to obtain a time-dependent solution of the SERR for the cantilever beam configuration depicted in Fig. 2. Then, the solution is used to determine the structural life. The length of the beam is l. The beam has a rectangular cross-section of width, b, and thickness, h. The length of the crack is a. The thicknesses of the lower and the upper crack arms are denoted by h_1 and h_2, respectively. The beam is clamped in its right-hand end. The external loading consists of one vertical force, F, applied at the free end of the lower crack arm (Fig. 2). Apparently, the upper crack arm is free of stresses. The beam is functionally graded along the thickness.

In this case the time-dependent solution of the SERR is derived by applying the general solution (1). The beam exhibits non-linear creep behavior that is treated by using the following non-linear stress-strain-time relationship (Rabinovich 1970)

$$\varepsilon = \frac{\sigma}{E} + \frac{t}{\eta}\sigma e^{\sigma\frac{3+\gamma}{3m}} \tag{35}$$

where E is the modulus of elasticity, η, γ and m are material properties which characterize the creep behavior. It should be noted that the first term in the right-hand side of (35) describes the instantaneous linear-elastic strain. The strain induced by the creep behavior is described by the second term in the right-hand side of (35).

The continuous distribution of the modulus of elasticity along the thickness of the beam is written as

$$E = E_{up}e^{s\frac{\frac{h}{2}+z}{h}} \tag{36}$$

where

$$-\frac{h}{2} \le z \le \frac{h}{2} \tag{37}$$

In formula (36), E_{up} is the value of the modulus of elasticity in the upper surface of the beam, s is a material property that controls the variation of E in the thickness direction, z is the vertical centroidal axis (Fig. 2).

By combining of (2), (3) and (35), one obtains the following time-dependent strain energy densities in the lower crack arm

$$u_{01}=\frac{\sigma^2}{E}+\frac{t}{\eta}\sigma^2 e^{g\sigma}-\frac{t}{\eta}\left[\ \frac{e^{\sigma g}}{g^2}(g\sigma-1)+\frac{1}{g^2}\ \right] \tag{38}$$

$$u_{01}^{*}=\frac{\sigma^2}{2E}+\frac{t}{\eta}\left[\ \frac{e^{\sigma g}}{g^2}(g\sigma-1)+\frac{1}{g^2}\ \right] \tag{39}$$

where $g=(3+\gamma)/(3m)$. In order to present the distribution of the modulus of elasticity along the thickness of the lower crack arm, (36) is re-written as

$$E=E_{up}e^{s\frac{z_1-\frac{h_1}{2}+h}{h}} \tag{40}$$

where

$$-\frac{h_1}{2}\le z_1\le\frac{h_1}{2} \tag{41}$$

By using (35), the function, $f(\sigma,t)$, is obtained as

$$f(\sigma,t)=\frac{\sigma}{E}+\frac{t}{\eta}\sigma\, e^{\sigma\frac{3+\gamma}{3m}}. \tag{42}$$

By substituting of (10), (40) and (42) in (13), (14) and (15), one derives

$$-\kappa_1 z_{1n}=\frac{\beta}{E_{up}e^{-q}}+\frac{t}{\eta}\beta e^{\beta g} \tag{43}$$

$$\kappa_1=\frac{\delta h-\beta s}{hE_{up}^{-q}}+\frac{t}{\eta}\delta e^{\beta g}+\frac{t}{\eta}\beta\delta g e^{\beta g} \tag{44}$$

$$0=\frac{2\eta h^2-2\delta s h+\beta s^2}{hE_{up}e^{-q}}+2te^{\beta g}+2t\beta g e^{\beta g}+\frac{t}{\eta}\beta\delta^2 g^2 e^{\beta}+2\frac{t}{\eta}\delta^2 g e^{\beta g}, \tag{45}$$

where $q=s(h_1+2h)/(2h)$. Eqs. (11), (12), (43), (44) and (45) are solved with respect to κ_1, z_{1n}, β, δ and η by using the MatLab computer program (it should be mentioned that the axial force and the bending moment which are involved in Eqs. (11) and (12) are obtained as $N_1=0$ and $M_1=Fx$ for the beam in Fig. 2). Then, the energy densities are found by substituting of (10) in (38) and (39).

The complementary strain energy in the upper crack arm is zero since the upper crack arm is free of stresses (Fig. 2).

The curvature, the coordinate of the neutral axis and the coefficients, β_{un}, δ_{un} and η_{un}, in the un-cracked beam portion ahead of the crack tip are found by using Eqs. (11), (12), (43), (44) and (45). For this purpose, κ_1, z_{1n}, β, δ and η are replaced with κ_3, z_{3n}, β_{un}, δ_{un} and η_{un}, respectively.

By substituting of the complementary strain energy densities in (1), the SERR is written as

$$G=\int_{-\frac{h_1}{2}}^{\frac{h_1}{2}} u_{01}^{*}dz_1-\int_{-\frac{h}{2}}^{\frac{h}{2}} u_{03}^{*}dz_3 \tag{46}$$

where the complementary strain densities are obtained by (11), (12), (39), (43), (44) and (45) at $x=a$. The integration in (46) is performed y using the MatLab computer program.

Time-dependent solution of the SERR for the cantilever beam shown in Fig. 2 is found also by considering the balance of the energy for verification of (46). For this purpose, the balance of the energy is written as

$$F\delta w=\frac{\partial U}{\partial a}\delta a+Gb\delta a \tag{47}$$

where w is the vertical displacement of the application point of the external force, U is the strain energy cumulated in the beam, δa is a small increase of the crack length. From (47), one obtains

$$G=\frac{F}{b}\frac{\partial w}{\partial a}-\frac{1}{b}\frac{\partial U}{\partial a}\ . \tag{48}$$

The vertical displacement of the application point of the external force is derived by applying the integrals of Maxwell-Mohr. The result is

$$w=\int_0^a \kappa_1 x dx+\int_a^l \kappa_3 x dx \tag{49}$$

where x is the longitudinal centroidal axis of the beam (Fig. 2). The strain energy cumulated in the beam is written as

$$U=U_1+U_3 \tag{50}$$

where U_1 and U_3 are the strain energies in the lower crack arm and the un-cracked beam portion, respectively. The strain energy in the lower crack arm is found as

$$U_1=b\int_0^a\int_{-\frac{h_1}{2}}^{\frac{h_1}{2}} u_{01}dxdz_1\,. \tag{51}$$

The strain energy in the un-cracked beam portion is written as

$$U_3 = b\int_a^l \int_{-\frac{h}{2}}^{\frac{h}{2}} u_{03} dx dz_3 \tag{52}$$

where the complementary strain energy density in the un-cracked beam portion, u_{03}, is calculate by applying formula (38). For this purpose, σ is replaced with σ_{un}.

By substituting of (49)-(52) in (48), one obtains

$$G = \frac{F}{b}\left(\kappa_1 a - \kappa_3 a \right) - \int_{-\frac{h_1}{2}}^{\frac{h_1}{2}} u_{01} dz_1 + \int_{-\frac{h}{2}}^{\frac{h}{2}} u_{03} dz_3 \tag{53}$$

where the curvatures and the strain energy densities are found by (11), (12), (38), (43), (44) and (45) at $x = a$. The MatLab computer program is used to carry-out the integration in (53). The SERR obtained by (53) matches that calculated by (46). This fact is a verification of the solution of the SERR obtained for the case of beam with identical creep behavior in tension and compression.

4.2 Case of beam with asymmetrical creep behavior in tension and compression

Solution (16) is applied to obtain the SERR in this case. The non-linear stress-strain-time relationship (35) is re-written as

$$\varepsilon = \frac{\sigma_c}{E_c} + \frac{t}{\eta_c}\sigma_c e^{\sigma_c \frac{3+\gamma_c}{3m_c}} \tag{54}$$

and

$$\varepsilon = \frac{\sigma_t}{E_t} + \frac{t}{\eta_t}\sigma_t e^{\sigma_t \frac{3+\gamma_t}{3m_t}} \tag{55}$$

for compression and tension, respectively. In formulae (54) and (55), E_c and E_t are the moduli of elasticity, respectively, in compression and tension, η_c, γ_c and m_c are material properties which characterize the creep behavior in compression. The creep behavior in tension is characterized by η_t, γ_t and m_t.

The variations of E_c and E_t along the thickness of the beam are expressed, respectively, as

$$E_c = E_{upc} e^{s_c \frac{\frac{h}{2}+z}{h}} \tag{56}$$

and

$$E_t = E_{upt} e^{s_t \frac{\frac{h}{2}+z}{h}} \tag{57}$$

where

$$-\frac{h}{2} \le z \le \frac{h}{2} \tag{58}$$

In formulae (56) and (57), E_{upc} and E_{upt} are the values of the moduli of elasticity in compression and tension at the upper surface of the beam, respectively. The material properties, s_c and s_t, control the variation of E_c and E_t along the thickness of the beam, respectively.

By using (38) and (39), the strain energy densities in the compression and tension zones in the lower crack arm are written, respectively, as

$$u_{01c} = \frac{\sigma_c^2}{E_c} + \frac{t}{\eta_c}\sigma_c^2 e^{g_c\sigma_c} - \frac{t}{\eta_c}\left[\frac{e^{\sigma_c g_c}}{g_c^2}(g_c\sigma_c - 1) + \frac{1}{g_c^2} \right]$$
$$u_{01c}^{*} = \frac{\sigma_c^2}{2E_c} + \frac{t}{\eta_c}\left[\frac{e^{\sigma_c g_c}}{g_c^2}(g_c\sigma_c - 1) + \frac{1}{g_c^2} \right] \tag{59}$$

$$u_{01t} = \frac{\sigma_t^2}{E_t} + \frac{t}{\eta_t}\sigma_t^2 e^{g_t\sigma_t} - \frac{t}{\eta_t}\left[\frac{e^{\sigma_t g_t}}{g_t^2}(g_t\sigma_t - 1) + \frac{1}{g_t^2} \right]$$
$$u_{01t}^{*} = \frac{\sigma_t^2}{2E_t} + \frac{t}{\eta_t}\left[\frac{e^{\sigma_t g_t}}{g_t^2}(g_t\sigma_t - 1) + \frac{1}{g_t^2} \right] \tag{60}$$

where $g_c = (3+\gamma_c)/(3m_c)$, $g_t = (3+\gamma_t)/(3m_t)$. By using (54) and (55), functions, $f(\sigma_c, t)$ and $f(\sigma_t, t)$, are written as

$$f(\sigma_c, t) = \frac{\sigma_c}{E_c} + \frac{t}{\eta_c}\sigma_c\, e^{\sigma_c \frac{3+\gamma_c}{3m_c}} \tag{61}$$

and

$$f(\sigma_t, t) = \frac{\sigma_t}{E_t} + \frac{t}{\eta_t}\sigma_t\, e^{\sigma_t \frac{3+\gamma_t}{3m_t}} \tag{62}$$

$$E_c = E_{upc} e^{s_c \frac{z_1 - \frac{h_1}{2} + h}{h}} \tag{63}$$

and

$$E_t = E_{upt} e^{s_t \frac{z_1 - \frac{h_1}{2} + h}{h}} \tag{64}$$

where

$$-\frac{h_1}{2} \le z_1 \le \frac{h_1}{2}. \tag{65}$$

By substituting of (23), (24), (61), (62), (63) and (64) in (29)-(34), one derives

$$\kappa_1(z_{1c} - z_{1n}) = \frac{\beta_c}{E_{upc} e^{\frac{s_c}{h} z_{1c} - q_c}} + \frac{t}{\eta_c}\beta_c e^{\beta_c g_c} \tag{66}$$

$$\kappa_1=\frac{\delta_c h-\beta_c s_c}{hE_{upc}^{s_c\frac{z_{1c}}{h}-q_c}}+\frac{t}{\eta_c}\delta_c e^{\beta_c g_c}+\frac{t}{\eta_c}\beta_c\delta_c g_c e^{\beta_c g_c} \tag{67}$$

$$0=\frac{2\eta_c h^2-2\delta_c s_c h+\beta_c s_c^2}{hE_{upc}e^{\frac{s_c}{h}z_{1c}-q_c}}+2te^{\beta_c g_c}+2t\beta_c g_c e^{\beta_c g_c}+\frac{t}{\eta_c}\beta_c\delta_c^2 g_c^2 e^{\beta_c g_c}+2\frac{t}{\eta_c}\delta_c^2 g_c e^{\beta_c g_c} \tag{68}$$

$$\kappa_1(z_{1t}-z_{1n})=\frac{\beta_t}{E_{upt}e^{\frac{s_t}{h}z_{1t}-q_t}}+\frac{t}{\eta_t}\beta_t e^{\beta_t g_t} \tag{69}$$

$$\kappa_1=\frac{\delta_t h-\beta_t s_t}{hE_{upt}^{s_t\frac{z_{1t}}{h}-q_t}}+\frac{t}{\eta_t}\delta_t e^{\beta_t g_t}+\frac{t}{\eta_t}\beta_t\delta_t g_t e^{\beta_t g_t} \tag{70}$$

$$0=\frac{2\eta_t h^2-2\delta_t s_t h+\beta_t s_t^2}{hE_{upt}e^{\frac{s_t}{h}z_{1t}-q_t}}+2te^{\beta_t g_t}+2t\beta_t g_t e^{\beta_t g_t}+\frac{t}{\eta_t}\beta_t\delta_t^2 g_t^2 e^{\beta_t g_t}+2\frac{t}{\eta_t}\delta_t^2 g_t e^{\beta_t g_t} \tag{71}$$

where $q_c=s_c(h_1+2h)/(2h)$, $q_t=s_t(h_1+2h)/(2h)$. Eqs. (27), (28), (66)-(71) are solved with respect to κ_1, z_{1n}, β_c, δ_c, η_c, β_t, δ_t and η_t by using the MatLab computer program (the axial force and the bending moment which are involved in Eqs. (27) and (28) are written as $N_1=0$ and $M_1=Fx$).

Equations (27), (28), (66) – (71) are used also to determine κ_3, z_{3n}, β_{unc}, δ_{unc}, η_{unc}, β_{unt}, δ_{unt} and η_{unt}. For this purpose, κ_1, z_{1n}, β_c, δ_c, η_c, β_t, δ_t and η_t are replaced with κ_3, z_{3n}, β_{unc}, δ_{unc}, η_{unc}, β_{unt}, δ_{unt} and η_{unt}, respectively.

The following expression for the SERR is found by substituting of the complementary strain energy densities in (16)

$$G=\int_{-\frac{h_1}{2}}^{z_{1n}}u_{01c}^{*}dz_1+\int_{z_{1n}}^{\frac{h_1}{2}}u_{01t}^{*}dz_1-\int_{-\frac{h}{2}}^{z_{3n}}u_{03c}^{*}dz_3-\int_{z_{3n}}^{\frac{h}{2}}u_{03t}^{*}dz_3. \tag{72}$$

The MatLab computer program is used to perform the integration in (72). The complementary strain energy densities which are involved in (72) are determined by using (27), (28), (59), (60), (66)-(71) at $x=a$.

In order to verify solution (72), the SERR is derived also by considering the balance of the energy. For this purpose, formula (48) is applied. The strain energy in the lower crack arm is written as

$$U_1=b\int_0^a\int_{-\frac{h_1}{2}}^{z_{1n}}u_{01c}dxdz_1+b\int_0^a\int_{z_{1n}}^{\frac{h_1}{2}}u_{01t}dxdz_1. \tag{73}$$

The complementary strain energy densities in the compression and tension, u_{01c} and u_{01t}, which are involved in (73) are obtained by (59) and (60). The strain energy in the un-cracked portion of the beam is found as

$$U_3 = b\int_a^l \int_{-\frac{h}{2}}^{z_{3n}} u_{03c}\,dx dz_3 + \int_a^l \int_{z_{3n}}^{\frac{h}{2}} u_{03t}\,dx dz_3, \tag{74}$$

where u_{03c} and u_{03t} are obtained by replacing of σ_c, σ_t and ε with σ_{unc}, σ_{unt} and ε_{un} in (59) and (60).

By substituting of (49), (50), (73) and (74) in (48), one derives

$$G = \frac{F}{b}\left(\kappa_1 a - \kappa_3 a\right) - \int_{-\frac{h_1}{2}}^{z_{1n}} u_{01c}\,dz_1 - \int_{z_{1n}}^{\frac{h_1}{2}} u_{01t}\,dz_1 + \int_{-\frac{h}{2}}^{z_{3n}} u_{03c}\,dz_3 + \int_{z_{3n}}^{\frac{h}{2}} u_{03t}\,dz_3 \tag{75}$$

where the curvatures and the strain energy densities are found by (27), (28), (59), (60), (66)-(71) at $x = a$. The integration in (53) is carried-out by the MatLab computer program. The fact that the SERR obtained by (53) matches that found by (72) verifies the solution for the case of beam with asymmetrical creep behavior in tension and compression.

It should be mentioned that the Maclaurin and Taylor series expansions up to higher order inclusive are also used. It is found that using order inclusive higher than the second order practically does not change the result (the difference is less than 2%). When higher-order terms are included, enough equations can be composed by substituting of $z_1 = 0$ in the third, fourth, etc. derivatives of (8). If higher-order terms are included when the creep behavior is asymmetric, enough equations can be obtained by substitution of $z_1 = z_{1c}$ in the third, fourth, etc. derivatives of (21). Analogically, $z_1 = z_{1t}$ has to be substituted in the third, fourth, etc. derivatives of (22).

4.3 Determining of the structural life

The results presented here are obtained by applying the time-dependent solutions of the SERR for the functionally graded cantilever beam (Fig. 2) derived in the previous section of the paper.

It is shown how the solutions can be used for determining the structural life of the cantilever beam with a longitudinal crack. The SERR is expressed in a non-dimensional form by using the formula $G_N = G/(E_{up}b)$. The variation of the SERR with the time is studied (this is necessary for determination of the structural life). The influence of the loading, the beam geometry, the crack length and asymmetrical creep behavior of the beam in tension and compression on the structural life is analyzed. It is assumed that $b = 0.020$ m, $l = 0.300$ m, $s = 0.4$, $s_c = 0.5$, $s_t = 0.6$, $h_1/h = 0.5$ and $F = 5$ N.

One can get an idea about the variation of the SERR with the time induced by the beam creep behavior from Fig. 3 where the SERR in non-dimensional form is plotted against the non-dimensional time. The plots in Fig. 3 are for beam with identical creep behavior in tension and compression. It should be mentioned that the SERR at $t = 0$ in Fig. 3 is due to the instantaneous linear-elastic reaction of the beam that is described by the first term in the right-hand side of (35). In order to examine the effect of loading, plots at three magnitudes of the force, F, are shown in Fig. 3. Besides, Fig. 3 illustrates the approach used for determining the structural life of the cantilever. In this paper, it is assumed that structural life of the beam with longitudinal crack is limited by the time for beginning of the crack growth. Therefore, for determining the structural life

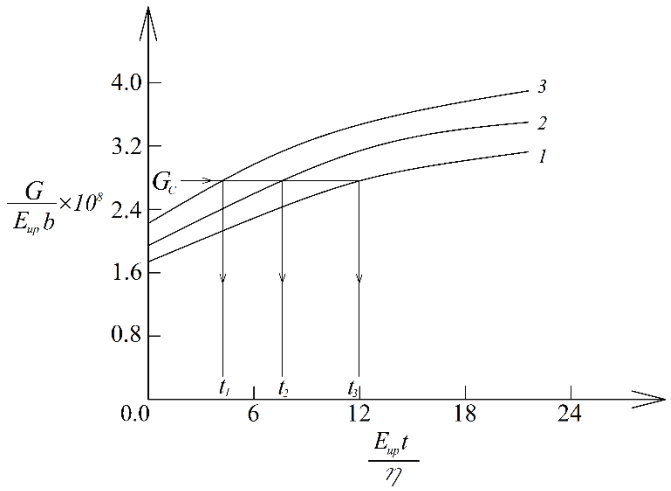

Fig. 3 The SERR in non-dimensional form plotted vs. the non-dimensional time (curve 1 - at $F=3$ N, curve 2 - at $F=4$ N and curve 3 - at $F=5$ N). The structural life at the different force magnitudes is denoted by t_1, t_2, and t_3

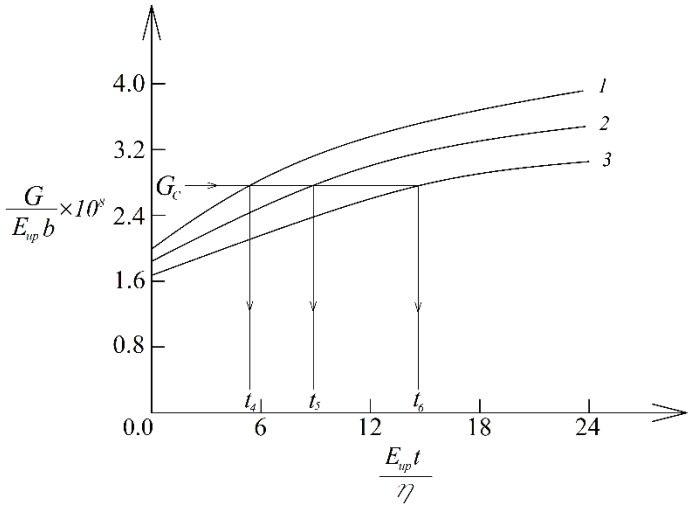

Fig. 4 Variation of the non-dimensional SERR with the non-dimensional time (curve 1 – at $h/b=1.2$, curve 2 – at $h/b=1.5$ and curve 3 – at $h/b=1.8$). The corresponding structural life of the cantilever beam is denoted by t_4, t_5, and t_6

we have to obtain the time for beginning of the crack growth. The time at which the SERR gets in line with the fracture toughness, G_C, is the time for beginning of the crack growth (Fig. 3).

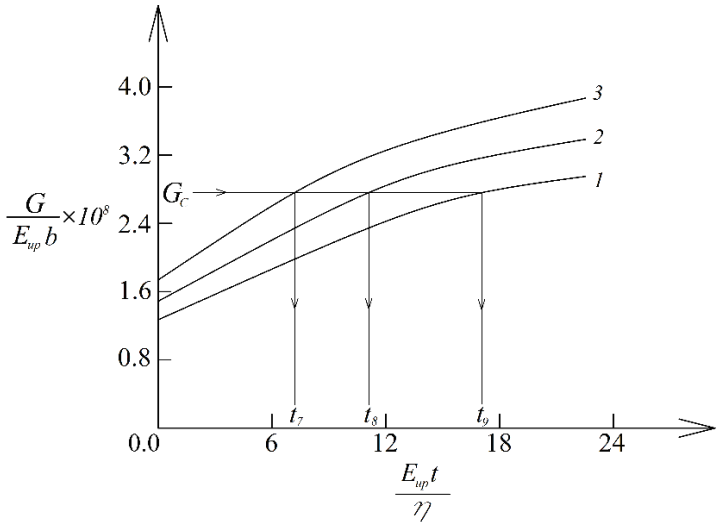

Fig. 5 Curves illustrating change of the non-dimensional SERR with the non-dimensional time (curve 1 – at $a/l=0.3$, curve 2 – at $a/l=0.5$ and curve 3 – at $a/l=0.7$). The structural life of the cantilever beam at different a/l ratios is denoted by t_7, t_8, and t_9

By using this approach, we determine the cantilever beam structural life denoted by t_1, t_2, and t_3 at the three vales of F as shown in Fig. 3.

The curves in Fig. 3 indicate that the structural life decreases with increasing of the force magnitude. This finding is attributed to the increase of the SERR induced by increase of the force acting on the beam.

The influence of the beam geometry (the latter is characterized by h/b ratio) on the structural life is analyzed too. In this relation, the SERR in non-dimensional form is plotted against the non-dimension time at three h/b ratios in Fig. 4. The plots in Fig. 4 are for a cantilever with identical creep behavior in tension and compression. The cantilever beam structural life for the considered h/b ratios is denoted by t_4, t_5, and t_6, respectively (Fig. 4). It is evident from Fig. 4 that the structural life increases when h/b ratio increases. This behavior is explained by reduction of the SERR when h/b ratio increases.

The influence of the crack length (the latter is characterized by a/l ratio) on the cantilever structural life is also evaluated. Beam with identical creep behavior in tension and compression is considered. The SERR in non-dimensional form is plotted against the non-dimension time in Fig. 5 at three a/l ratios. It is obvious from Fig. 5 that the structural life reduces with increasing of a/l ratio. This is due to growth of the SERR generated by increase of a/l ratio (Fig. 5).

Finally, it is explored how the cantilever beam structural life is affected by asymmetrical creep behavior in tension and compression. For this purpose, variation of the non-dimensional SERR with the non-dimensional time for both cases (beam with identical creep behavior in tension and compression and beam with asymmetrical creep behavior in tension and compression) is shown in Fig. 6. It can be observed in Fig. 6 that the structural life of beam with asymmetrical creep behavior in tension and compression is shorter than that of beam with identical creep behavior in tension and compression.

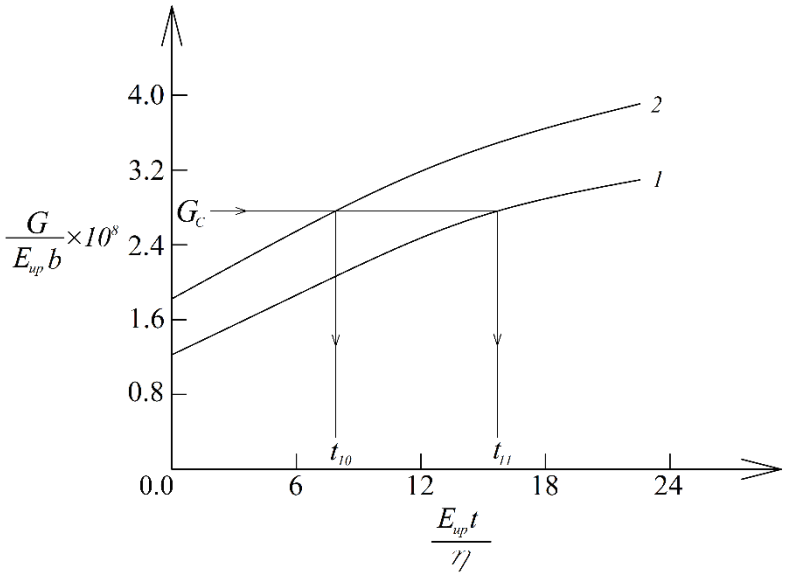

Fig. 6 The non-dimensional SERR presented as a function of the non-dimensional time (curve 1 – for the case of beam with identical creep behavior in tension and compression, curve 2 –for the case of beam with asymmetrical creep behavior in tension and compression). The structural life of the cantilever beam for the considered cases of creep behavior is denoted by t_{10} and t_{11}

The explanation of this finding is in growth of the SERR when the beam has asymmetrical creep behavior in tension and compression.

5. Conclusions

An approach for evaluation of the effect of longitudinal cracks on structural life of functionally graded beams exhibiting non-linear creep is developed. In this relation, general time-dependent solution of the SERR is derived. The crack is located arbitrary along the beam thickness (thus, the two crack arms have different thicknesses). The beam is functionally graded in the thickness direction (the continuous variation of material properties along the thickness is arbitrary). The creep behavior of the beam is treated by using non-linear stress-strain-time relationship in general form. Two cases (beams with identical creep behavior in tension and compression and beams with asymmetrical creep behavior in tension and compression) are considered. The general time-dependent solution of the SERR is applied for determining the structural life of a functionally graded cantilever beam with a longitudinal crack. Time-dependent solution of the SERR in the cantilever beam is obtained also by considering the energy balance for verification. It is found that the structural life reduces with increasing the magnitude of the external force. The analysis reveals that the structural life grows when h/b ratio increases. Growth of a/l ratio induces reduction of the structural life of the cantilever. It is observed that the structural life of the beam with asymmetrical creep behavior in tension and compression is shorter than that of the beam with identical creep behavior in tension and compression. The analysis performed indicates that the

approach represents a useful tool for determination of the structural life of functionally graded beams in which longitudinal cracks are observed during maintenance check. The practical application of the approach developed here proceeds through the following steps. First, the location and length of the longitudinal crack must be determined (usually by visual inspection of the beam structure). Then, by applying the approach, the evolution of the SERR with time due to creep must be analyzed. Finally, the service life of the structure can be determined by equating the SERR with the fracture toughness.

Acknowledgments

The first author (V. I. R.) is grateful to the German Academic Exchange Organization (DAAD) for supporting his research stay in Department of Engineering Mechanics, Institute of Mechanics, Otto-von-Guericke-University, Magdeburg, Germany.

References

Ait Atmane, H., Tounsi, A. and Bernard, F. (2017), "Effect of thickness stretching and porosity on mechanical response of a functionally graded beams resting on elastic foundations", *Int. J. Mech. Mater. Design*, **13**(1), 71-84. https://doi.org/10.1007/s10999-015-9318-x.

Al-Shablle, M., Al-Waily, M. and Njim, E.K. (2022), "Analytical evaluation of the influence of adding rubber layers on free vibration of sandwich structure with presence of nano-reinforced composite skins", *Arch. Mater. Sci. Eng.*, **116**(2), 57-70. https://doi.org/10.5604/01.3001.0016.1190.

Daouadji, T.H., Chedad, A. and Adim, B. (2016), "Interfacial stresses in RC beam bonded with a functionally graded material plate", *Struct. Eng. Mech.*, **60**(4), 693-705. https://doi.org/10.12989/sem.2016.60.4.693.

Dolgov, M.A. (2024), "Analysis of the stress state in the deformed coating under Base Stretching with the Bending Effect Account", *Strength Mater*, **56**, 1127-1135. https://doi.org/10.1007/s11223-025-00723-2.

Dowling, N.E. (2013), *Mechanical behaviour of materials*, Person.

Gasik, M.M. (2010), "Functionally graded materials: bulk processing techniques", *Int. J. Mater. Product Technol.*, **39**(1-2), 20-29. https://doi.org/10.1504/IJMPT.2010.034257.

Hirai, T. and Chen, L. (1999), "Recent and prospective development of functionally graded materials in Japan", *Mater. Sci. Forum*, **308-311**(4), 509-514. https://doi.org/10.4028/www.scientific.net/MSF.308-311.509.

Kadum Njim, E., Al-Maamori, M.H., Madan, R., Bakhy, S.H., Al-Waily, M., Khobragade, P. and Hadji, L. (2025), "Numerical and analytical investigation of free vibration behavior of porous functionally graded sandwich plates", *Mech. Adv. Compos. Struct.*, **12**(3), 555-568. https://doi.org/10.22075/MACS.2024.34962.1710.

Mahamood, R.M. and Akinlabi, E.T. (2017), *Functionally Graded Materials*, Springer.

Markworth, A.J., Ramesh, K.S. and Parks, Jr. W.P. (1995), "Review: modeling studies applied to functionally graded materials", *J. Mater. Sci.*, **30**(3), 2183-2193. https://doi.org/10.1007/BF01184560.

Miyamoto, Y., Kaysser, W.A., Rabin, B.H., Kawasaki, A. and Ford, R.G. (1999), *Functionally Graded Materials: Design, Processing and Applications*, Kluwer Academic Publishers, Dordrecht/London/Boston.

Nemat-Allal, M.M., Ata, M.H., Bayoumi, M.R. and Khair-Eldeen, W. (2011), "Powder metallurgical fabrication and microstructural investigations of Aluminum/Steel functionally graded material", *Mater. Sci. Appl.*, **2**(5), 1708-1718. https://doi.org/10.4236/msa.2011.212228.

Nguyen, S.N., De Pascalis, R., Yousaf, Z. and Parnell, W.J. (2025), "All-polymer syntactic foams: Linking

large strain cyclic experiments to Quasilinear Viscoelastic modelling for materials characterisation", *Compos. Part B: Eng*., **288**, 111866. https://doi.org/10.1016/j.compositesb.2024.111866.
Nguyen, S.N., Lee, J. and Cho, M. (2015), "Efficient higher-order zig-zag theory for viscoelastic laminated composite plates", *Int. J. Solids Struct.*, **62**, 174-185**.** https://doi.org/doi.org/10.1016/j.ijsolstr.2015.02.027**.**
Nguyen, S.N., Lee, J., Han, J.W. and Cho, M. (2020), "A coupled hygrothermo-mechanical viscoelastic analysis of multilayered composite plates for long-term creep behaviors", *Compos. Struct.*, **242**, 112030. https://doi.org/10.1016/j.compstruct.2020.112030.
Njim, E.K., Al-Waily, M. and Bakhy, S.H. (2021), "A critical review of recent research of free vibration and stability of functionally graded materials of sandwich plate", *IOP Conf. Series: Materials Science and Engineering*, **1094**, 012081. https://doi.org/10.1088/1757-899X/1094/1/012081.
Njim, E.K., Bakhy, S.H. and Al-Waily, M. (2021), "Free vibration analysis of imperfect functionally graded sandwich plates: analytical and experimental investigation", *Arch. Mater. Sci. Eng.*, **111**(2), 49-65. https://doi.org/10.5604/01.3001.0015.5805.
Rabinovich, A.L. (1970), *Introduction to mechanics of reinforced polymers*, Science.
Rizov, V. (2025), "Longitudinal fracture analysis of continuously inhomogeneous beams undergoing general planar motion", *J. Appl. Comput. Mech.*, https://doi.org/10.22055/jacm.2025.48102.4977.
Rizov, V.I. (2020), "Influence of the viscoelastic material behaviour on the delamination in multilayered beam", *Procedia Struct. Integrity*, **25**, 88-100. https://doi.org/10.1016/j.prostr.2020.04.013.
Rizov, V.I. (2020), "Longitudinal fracture analysis of inhomogeneous beams with continuously changing radius of cross-section along the beam length", *Strength, Fracture and Complexity: An International Journal,* **13**, 31-43 https://doi.org/10.3233/SFC-200250.
Rizov, V.I. (2022), "Effects of periodic loading on longitudinal fracture in viscoelastic functionally graded beam structures", *J. Appl. Comput. Mech*., **8**(1), 370-378. https://doi.org/10.22055/JACM.2021.37953.3141.
Rizov, V.I. (2024), "The effect of delamination between layers in U-shaped members made of functionally graded multilayered viscoelastic materials", *J. Appl. Comput. Mech.*, **10**, 830-841. https://doi.org/10.22055/jacm.2024.46014.4449.
Rizov, V.I. and Altenbach, H. (2019), "On the analysis of lengthwise fracture of functionally graded round bars", *Struct. Integrity life*, **19**(2), 102-108. UDC:66.017/.018.539.42.
Sadoun, Z., Bennai, R., Nebab, M., Dahmane, M. and Ait Atmane, H. (2023), "Investigation of the behavior of an RC beam strengthened by external bonding of a porous P-FGM and E-FGM plate in terms of interface stresses", *Struct. Monit. Maint.*, **10**(4), 315-337. doi.org/10.12989/smm.2023.10.4.315.
Saiyathibrahim, A., Subramaniyan, R. and Dhanapl, P. (2016), "Centrefugally cast functionally graded materials – review", *Proceedings of the International Conference on Systems, Science, Control, Communications, Engineering and Technology*, 68-73.
Tokovyy, Y. (2019), "Solutions of axisymmetric problems of elasticity and thermoelasticity for an inhomogeneous space and a half space", *J. Math. Sci.*, **240**(1), 86-97. https://doi.org/10.1007/s10958-019-04337-3.
Tokovyy, Y. and Ma, C.C. (2017), "Three-dimensional elastic analysis of transversely-isotropic composites", *J. Mech.*, **33**(6), 821-830. https://doi.org/10.1017/jmech.2017.91.
Tokovyy, Y. and Ma, C.C. (2019), "Elastic analysis of inhomogeneous solids: History and development in brief", *J. Mech.*, **18**(1), 1-14. https://doi.org/10.1017/jmech.2018.57.
Tokovyy, Y. and Ma, C.C. (2021), *The direct integration method for elastic analysis of nonhomogeneous solids*, Cambridge Scholars Publishing.
Tokovyy, Y., Kulchytskyi-Zhyhailo, Y. and Huang, S. (2025), "Thermostressed analysis of multilayer elastic spherical vessels using the homogenized and multilayer models", *J. Therm. Stresses*, 1-25. https://doi.org/10.1080/01495739.2025.2477554.
Tokovyy, Y.V. (2023), "Elastic and thermoelastic response of multilayer inhomogeneous hollow cylinders", *Mech. Adv. Mater. Struct.*, **31**(17), 3889-3901. https://doi.org/10.1080/15376494.2023.2186548.
Truong, V.H., Le, Q.H., Lee, J., Han, J.W., Tessler, A. and Nguyen, S.N. (2024), "An efficient neural network approach for laminated composite plates using refined zigzag theory", *Compos. Struct.*, **34**,

118476. https://doi.org/10.1016/j.compstruct.2024.118476.
Udupa, G., Rao, S.S. and Gangadharan, K.V. (2014), "Functionally graded composite materials: An overview", *Procedia Mater. Sci.*, **5**(1), 1291-1299. https://doi.org/10.1016/j.mspro.2014.07.442.
Wu, X.L., Jiang, P., Chen, L., Zhang, J.F., Yuan, F.P. and Zhu, Y.T. (2014), "Synergetic strengthening by gradient structure", *Mater. Res. Lett*., **2**(1), 185-191. https://doi.org/10.1080/21663831.2014.935821.
Yousef, A.M., Abd El-Hady, K. and El-Madawy, M.E. (2022), "Prediction of ultimate shear strength and failure modes of R/C ledge beams using machine learning framework", *Struct. Monit. Maint.*, **9**(4), 337-357. https://doi.org/10.12989/smm.2022.9.4.337.

TY